Journal of Zhejiang University-SCIENCE A

Thin film bulk acoustic wave filters with ring-dot electrodes

Jing LIU, Jian-ke DU, Ji WANG, Jia-shi YANG

Key words: Piezoelectric; Thin film; Vibration; Resonator; Filter

Cite this as: Jing LIU, Jian-ke DU, Ji WANG, Jia-shi YANG, 2018. Thin film bulk acoustic wave filters with ring-dot electrodes. *Journal of Zhejiang University-SCIENCE A (Applied Physics & Engineering)*, 19(10):786-795. https://doi.org/10.1631/jzus.A1700396

Application

Comparison with SAW & Ceramics			
	FBAR	SAWs	ceramics
Frequency	400 MHz to 10 GHz	1 MHz to 2 GHz	1 MHz to 10 GHz
Size	Semiconductor (acoustic)	Semiconductor (acoustic)	Quarter wave (electric)
Q	1000	100s	100s
Temp Co	20 to 30 ppm/C	35 to 90 ppm/C	0 to 5 ppm/C
Power	> 1 W	< 1W	>>1 W

Table 1: AVAGO FBAR comparison with SAW and Ceramics

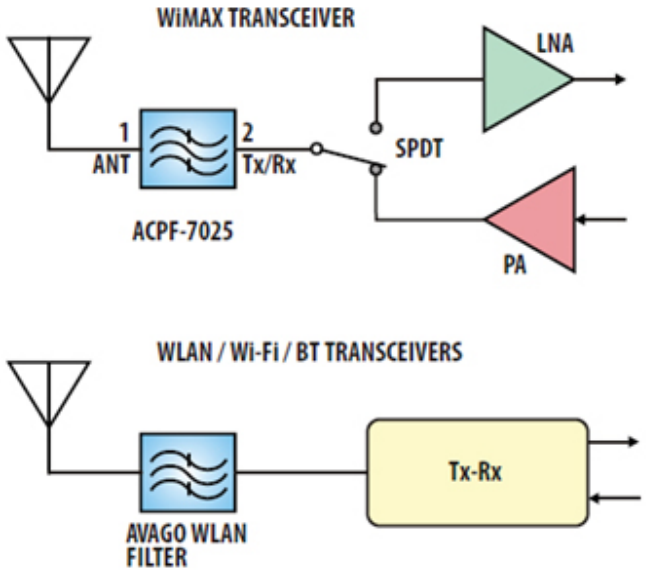

Figure 1: Typical multi system block diagram

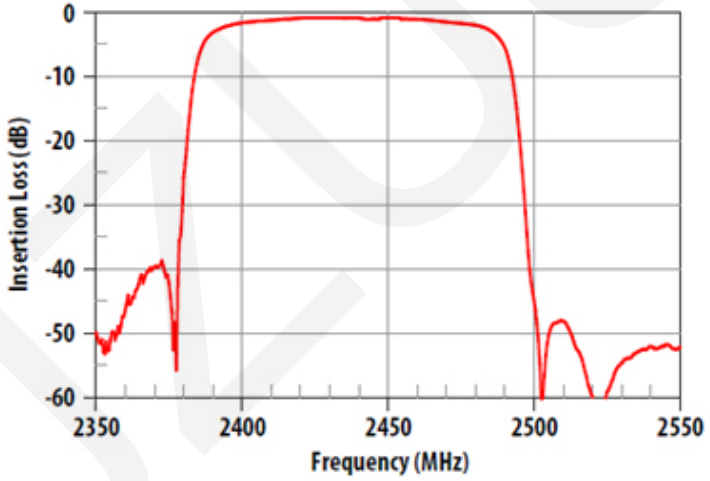

Figure 2: ACPF-7024 out of band attenuation 2350-2550MHz

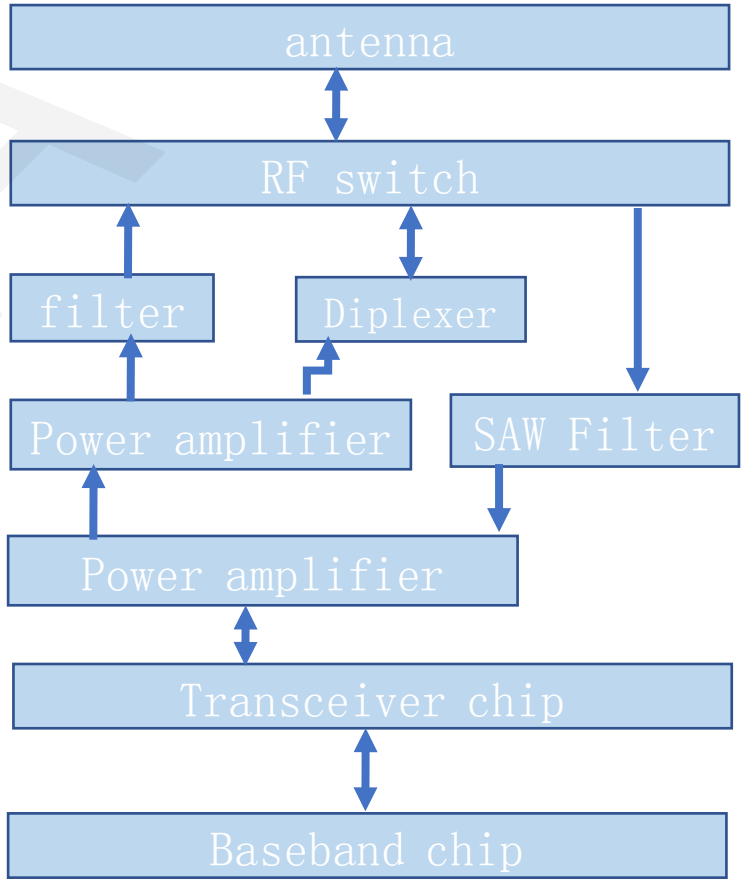

Figure 3: Filters play an important Role in RF front-end

Governing Equation

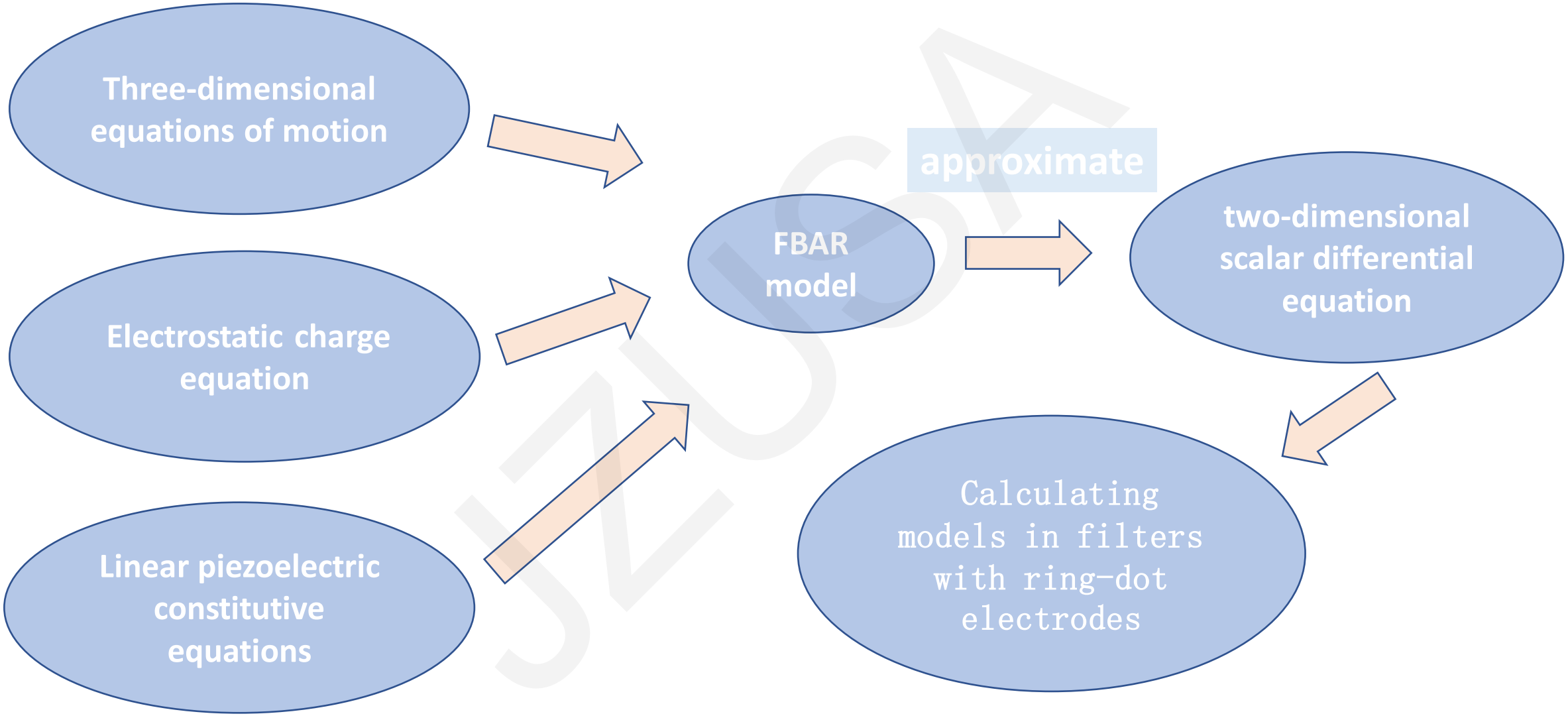

Scalar Equations

Mechanics Model

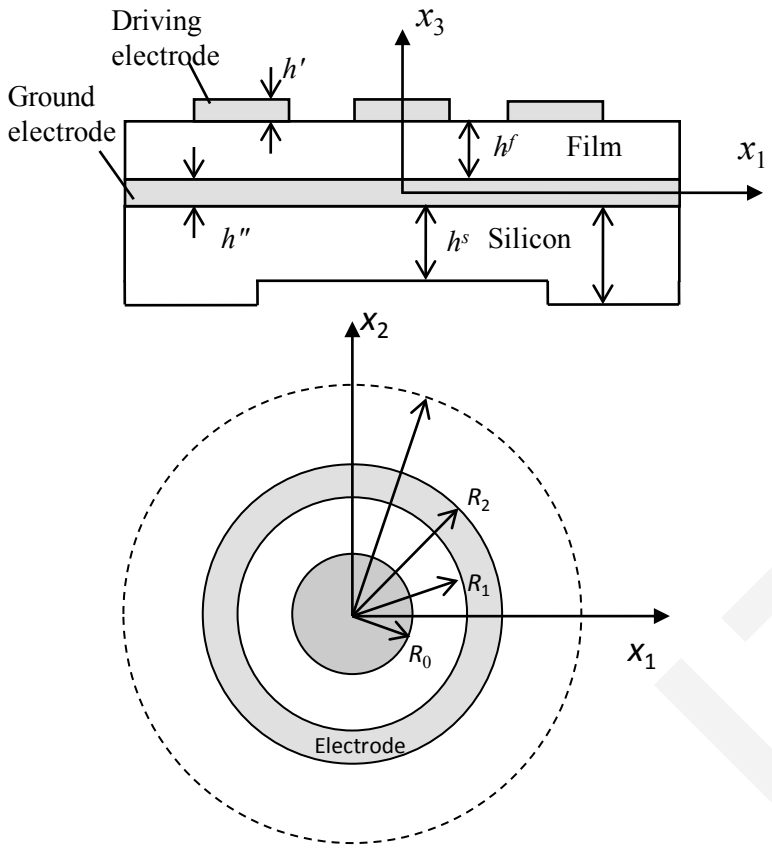

Figure 4: The lateral view and top view of a thin film bulk acoustic wave filter with ring-dot electrodes

Tiersten-Stevens two-dimensional scalar differential equation:

$$M_n\left(\frac{\partial^2 u_3^{f^n}}{\partial x_1^2}+\frac{\partial^2 u_3^{f^n}}{\partial x_2^2}\right)-\bar{c}_{33}^f\tilde{\eta}_{f^n}^2 u_3^{f^n}-\rho^f\ddot{u}_3^{f^n}=0,$$

$$0<x_3<h^f.$$

$$M_n\left(\frac{\partial^2 u_3^{s^n}}{\partial x_1^2}+\frac{\partial^2 u_3^{s^n}}{\partial x_2^2}\right)-\bar{c}_{33}^f\tilde{\eta}_{f^n}^2 u_3^{s^n}-\rho^f\ddot{u}_3^{s^n}=0,$$

$$0>x_3>-h^s.$$

$$u_3^{f^n}=\left(A_3^{s1n}\cos\eta_{s^n}^0 x_3+B_3^{s1n}\sin\eta_{s^n}^0 x_3\right)f^n(x_1,x_2,t),$$

$$0>x_3>-h^s.$$

$$u_3^{f^n}=\left(A_3^{f1n}\cos\eta_{f^n}^0 x_3+B_3^{f1n}\sin\eta_{f^n}^0 x_3\right)f^n(x_1,x_2,t),$$

$$0<x_3<h^f.$$

JZUSA

Numerical Results

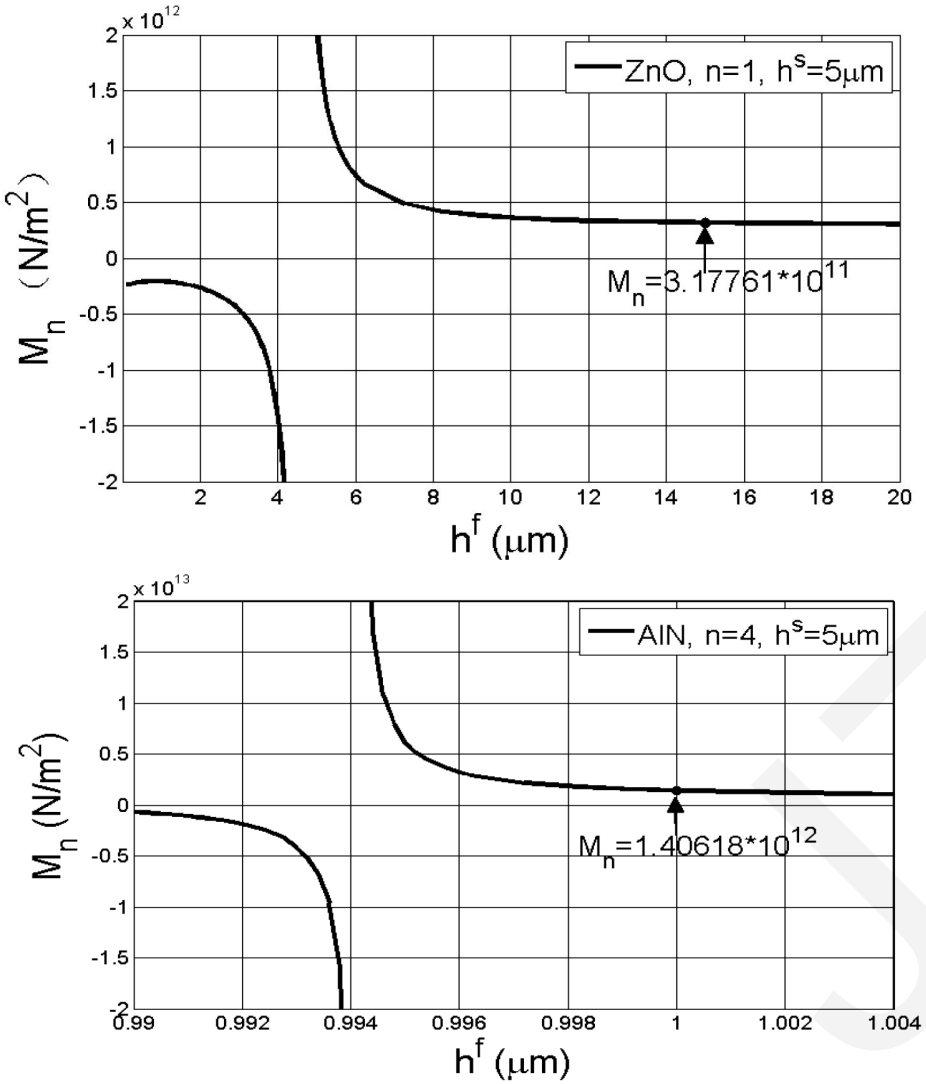

Figure 5: Mn for (a) ZnO on Si with *n*=1, and (b) AlN on Si with *n*=4.

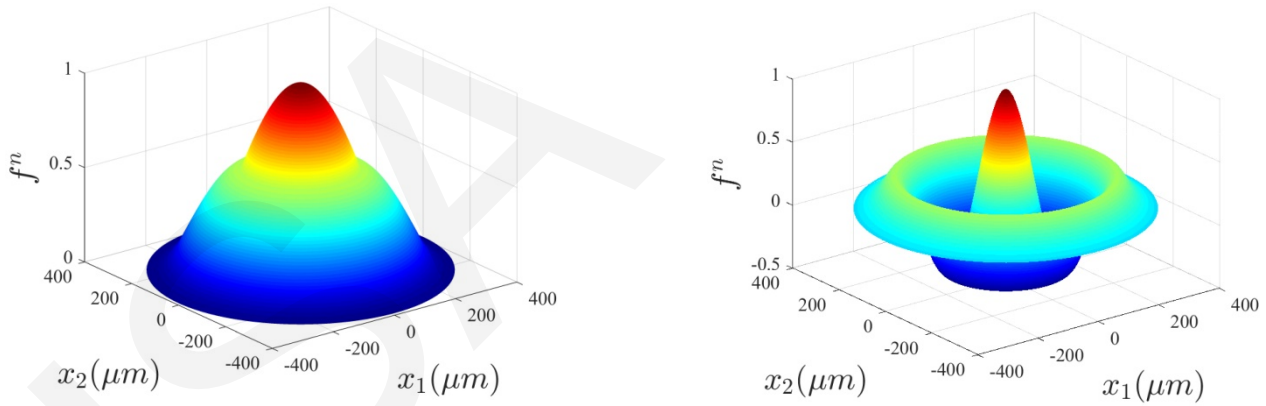

Figure 6: Two trapped thickness-extensional modes. (a) f_1=365.5336 MHz (b) f_2=367.4778 MHz

R_0 (μm)	R_1 (μm)	R_2 (μm)	h' (μm)	ρ' (g/m^3)	$(f_1+f_2)/2$ (MHz)	f_2-f_1 (kHz)
150	160	320	0.044	19.3	366.5057	1944.2528
130	160	320	0.044	19.3	366.8929	1331.3685
120	160	320	0.044	19.3	367.0877	1260.6349
150	170	320	0.044	19.3	366.6965	1600.5770
150	180	320	0.044	19.3	366.8634	1402.4924
150	160	350	0.044	19.3	366.2283	1641.4400
150	160	400	0.044	19.3	365.9003	1349.9358
150	160	320	0.200	19.3	349.6776	1718.8152
150	160	320	0.400	19.3	327.9103	1534.1840
150	160	320	0.044	10.2	368.7126	1959.9168
150	160	320	0.044	2.7	370.5160	1956.7986

Table 2 Average frequency and frequency difference of the operating modes

Conclusions

- Within the narrow frequency interval , there exist a few trapped modes with vibrations mainly under the dot-ring electrodes.
- With proper design, the nodal line of the second trapped mode lies in the gap between the ring and the dot electrodes. Then the first two trapped modes of the proposed structure can be used as the ideal operating modes for a filter.
- The location of the nodal line and the decay rate of the fields away from the electrode edges are sensitive to geometric and physical parameters.

JZUSA